REMOTE SENS. ENVIRON. 40:197-218 (1992)

Polynomial Trend Surface Analysis Applied to AVHRR Images to Improve Definition of Arctic Leads

Duane T. Eppler

Naval Oceanographic and Atmospheric Research Laboratory, Hanover, New Hampshire

William E. Full

FIMTSI, Department of Geology, Wichita State University

Polynomial trend surface analysis was applied to three AVHRR images to determine whether regional trends in image radiance can be removed with this procedure. Results suggest that trend surface techniques can be effective in removing region-scale variation in image radiances that are related to uneven illumination, intermittent cloud cover, and variation in the surface temperature field. The dominant effects of illumination in Channel 2 (visible) data, caused by variable sun angle and proximity of the scene to the terminator, can be minimized by removing (subtracting) the first- and second-order trend surfaces from the raw image. These low-order surfaces also remove regional variation in the surface temperature field, which leads to marginal improvement in binary images derived from Channel 4 (infrared) data. Optimum results for both Channel 2 and Channel 4 data are achieved when the third- and fourth-order surfaces are subtracted to remove local temperature and illumination anomalies that occur at smaller spatial scales, primarily in the vicinity of clouds. Application of higher order surfaces fails to improve image quality. There is some indication that the topography of these higher-order surfaces in part maps regional variation in lead density. Use of a best-fit criterion based on a strict variance technique (such as the least-squares method) to define the trend surface limits the effectiveness of the technique in this application. Criteria that allow for data to be weighted based on their distance from the plane about which they cluster are more appropriate to the structure of AVHRR radiance data typical of images that show sea ice. A criterion that incorporates a rule system based on fuzzy logic offers an alternative means of assessing goodness-of-fit that might prove appropriate in this application.

INTRODUCTION

Leads are cracks in the sea ice pack, typically linear in form, that initially expose sea water but commonly are frozen, especially during winter months. They are among the dominant features of the arctic sea ice pack readily observed from space with satellite sensors. Leads are important from a geophysical perspective for several reasons. Inasmuch as sea ice forms an insulating cover over warm ocean waters, leads provide the primary conduit through which heat exchanges with the cold atmosphere during winter months (Maykut, 1978; 1982; Smith et al., 1990). Brine rejected from freezing sea water in open leads

Address correspondence to Duane T. Eppler, NOARL Branch Office, Code 332, 72 Lyme Rd., Hanover, NH 03755-1290.

Received 29 April 1991; revised 18 January 1992.

0034-4257/92/$5.00

655 Avenue of the Americas, New York, NY 10010

initiates circulation in the mixed layer (Shaus and Galt, 1973; Kozo, 1983) and is believed to be a significant source of intermediate and deep water in the oceans (Martin and Cavalieri, 1989). Finally, lead patterns reflect deformation fields and, if studied through time-series imagery, signal changes in large scale motion of the ice pack. Leads thus are features of geophysical significance that are important to detect, monitor, and map.

Recent efforts to develop automated means of detecting and describing lead patterns have employed Hough transform methods (Duda and Hart, 1972; Wang and Howarth, 1989) applied to AVHRR (Advanced Very High Resolution Radiometer) scenes (Fetterer and Holyer, 1989; Fetterer et al., 1990). An essential requisite to extracting lead statistics using the Hough technique is a binary image (Fig. 1), derived from the original AVHRR scene using conventional thresholding (segmentation) techniques, in which pixels are classified as either leads or not leads based on their intensity. Individual lead elements must be portrayed accurately with respect to both width and continuity (or discontinuity) in these binary images if analytic methods (Hough transform or otherwise) are to produce accurate lead statistics.

Implicit in the use of binary segmentation methods is the assumption that radiances typical of the features of interest (leads and mature pack ice in this application) are uniform across the scene. If this requirement is not met, then the threshold value used to classify the scene is not appropriate everywhere in the image. In such case features will be defined well in some areas and not in others, as shown by the patchy, discontinuous nature of lead patterns in Figure 1. Few if any AVHRR images are characterized by radiances sufficiently uniform to satisfy this requirement, in large part because these scenes show such broad areas of the earth's surface (the AVHRR swath is 2900 km wide). Significant contributors to this nonuniformity include uneven surface illumination, region-scale changes in the surface- or air-temperature field, and the presence of thin clouds, all of which commonly vary on broad spatial scales, and all of which confound binary segmentation of leads using conventional level slicing techniques.

The objective of work described here is to evaluate use of polynomial trend surface methods

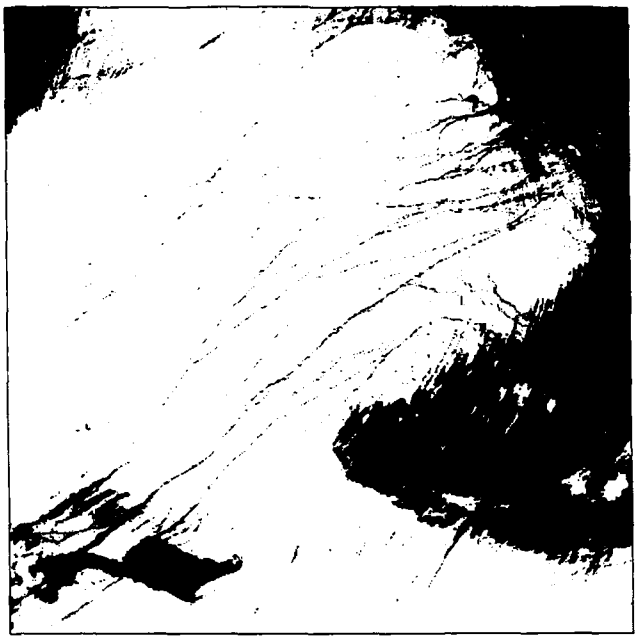

Figure 1. Binary image produced by segmenting an AVHRR Channel 4 (infrared) scene that shows sea ice, leads, and clouds. Standard level slicing techniques were used to produce the binary image. Leads appear as discontinuous lines that, in general, trend from upper right to lower left across the scene. Clouds along the right edge of the image appear black. Cloud structures manifest as arcuate wind streets are evident along the edge of the cloud mass. Lead signatures are defined poorly at the left edge of the image, and become more continuous towards the right side of the image as the cloud mass is approached. Application of the polynomial trend surface technique described here enhances leads and suppresses effects of clouds as shown by comparison of this image with the processed scene in Figure 10.

to model and to correct for broad-scale trends in radiance observed in AVHRR images. Polynomial trend surface analysis is a numeric technique that can be used to construct surfaces that represent best-fit estimates of mean variation in the height of a surface (Harbaugh and Merriam, 1968; Koch and Link, 1980; Davis, 1986). Here we use AVHRR image radiances to define the raw surface. In principle, a polynomial surface can be constructed to describe broad-scale trends in radiance, for example, the change in illumination observed near the terminator that separates night and day, that complicate automated classification or recognition of objects in a scene. Confounding effects of these unwanted artifacts, once captured in a polynomial surface, can be removed by subtracting the trend from the original image.

Here we report results of a pilot study designed to evaluate the effectiveness of polynomial

REPORT DOCUMENTATION PAGE

Form Approved
OBM No. 0704-0188

1. Agency Use Only *(Leave blank).*	2. Report Date.	3. Report Type and Dates Covered.
	1992	Final - Journal Article

4. Title and Subtitle.
Polynomial Trend Surface Analysis Applied to AVHRR Images to Improve Definition of Arctic Leads

5. Funding Numbers.

Contract	
Program Element No.	0601153N
Project No.	3205
Task No.	050
Accession No.	DN256025
Work Unit No.	13321D

6. Author(s).
Duane T. Eppler and William E. Full*

7. Performing Organization Name(s) and Address(es).
Naval Oceanographic and Atmospheric Research Laboratory
Polar Oceanography Branch
72 Lyme Road
Hanover, NH 03755-1290

8. Performing Organization Report Number.
JA 332:029:91

9. Sponsoring/Monitoring Agency Name(s) and Address(es).
Naval Oceanographic and Atmospheric Research Laboratory
Basic Research Management Office
Stennis Space Center, MS 39529-5004

10. Sponsoring/Monitoring Agency Report Number.
JA 332:029:91

11. Supplementary Notes.
Published in Remote Sens. Environ.
*FIMTSI, Department of Geology, Wichita State University

12a. Distribution/Availability Statement.
Approved for public release; distribution is unlimited.

12b. Distribution Code

13. Abstract *(Maximum 200 words).*
Polynomial trend surface analysis was applied to three AVHRR images to determine whether regional trends in image radiance can be removed with this procedure. Results suggest that trend surface techniques can be effective in removing region-scale variation in image radiances that are related to uneven illumination, intermittent cloud cover, and variation in the surface temperature field. The dominant effects of illumination in Channel 2 (visible) data, caused by variable sun angle and proximity of the scene to the terminator, can be minimized by removing (subtracting) the first- and second-order trend surfaces from the raw image. These low-order surfaces also remove regional variation in the surface temperature field, which leads to marginal improvement in binary images derived from Channel 4 (infrared) data. Optimum results for both Channel 2 and Channel 4 data are achieved when the third- and fourth-order surfaces are subtracted to remove local temperature and illumination anomalies that occur at smaller spatial scales, primarily in the vicinity of clouds. Application of higher order surfaces fails to improve image quality. There is some indication that the topography of these higher-order surfaces in part maps regional variation in lead density. Use of a best-fit criterion based on a strict variance technique (such as the least-squares method) to define the trend surface limits the effectiveness of the technique in this application. Criteria that allow for data to be weighted based on their distance from the plane about which they cluster are more appropriate to the structure of AVHRR radiance data typical of images that show sea ice. A criterion that incorporates a rule system based on fuzzy logic offers and alternative means of assessing goodness-of-fit that might prove appropriate in this application.

14. Subject Terms.
Sea ice classification. passive microwave, remote sensing

15. Number of Pages.
22

16. Price Code.

17. Security Classification of Report.	18. Security Classification of This Page.	19. Security Classification of Abstract.	20. Limitation of Abstract.
Unclassified	Unclassified	Unclassified	SAR

trend surface techniques as a means of improving binary segmentation of AVHRR images into lead and nonlead pixels in operational applications. Below we explain the trend surface technique and the manner in which we implement it. Following this, we describe results obtained when the method was applied to three AVHRR scenes. Finally we discuss limitations of the technique in this application, and possible modifications to the procedure that might improve its performance.

POLYNOMIAL TREND SURFACE ANALYSIS

Trend surface analysis is a mathematical technique that can be used to decompose a three-dimensional surface into a series of component surfaces that are defined by polynomial expansions of increasing order. The technique has been applied previously as a tool in mineral and petroleum exploration where it has been applied to analyze subsurface topography and to model regional trends in geophysical parameters. Expanded discussions of the technique, its implementation, and representative problems to which it has been applied are provided by Chorley and Haggett (1965), Harbaugh and Merriam (1968), King (1969), Chayes (1970), Doveton and Parsley (1970), Koch and Link (1980), and Davis (1986).

The two-dimensional algebraic analog to trend surface methods that define three-dimensional surfaces is regression analysis. Conventional linear regression procedures, for instance, fit a first-order equation to a data cloud plotted in x–y coordinate space using a least-squares criterion (Fig. 2A). Linear equations, which plot as straight lines, provide estimates of the first-order trend of the data in two dimensions. The position of the line with respect to the data cloud is optimized by adjusting coefficients that define the slope and the y-axis intercept of the line until the sum of squares of distances from the line to points in the cloud is minimized. If the shape of the data cloud is not linear, then a higher order equation (quadratic, cubic, and so forth) can be used to model the data (Fig. 2B). The term order refers to the highest power in any term in the equation that defines the best-fit curve. For example, a cubic equation contains a variable raised to the power of 3; hence it is referred to as a third-order equation.

Trend surface analysis in effect extends regression analysis from two-dimensional lines to three-dimensional surfaces. The technique uses a series of polynomial equations to define the best-fit, three-dimensional surface to data points plotted in x–y–z coordinate space, where x and y define a geographic coordinate and z records the radiance value at that location. A least-squares criterion (sum-of-squares of the distance from the surface to each point measured parallel to the z-axis) is used commonly to determine goodness-of-fit. Goodness-of-fit is a statistic which is used to measure how well the mathematical surface describes the average trend of the data.

The order of the polynomial that is used determines both the complexity of the best-fit surface

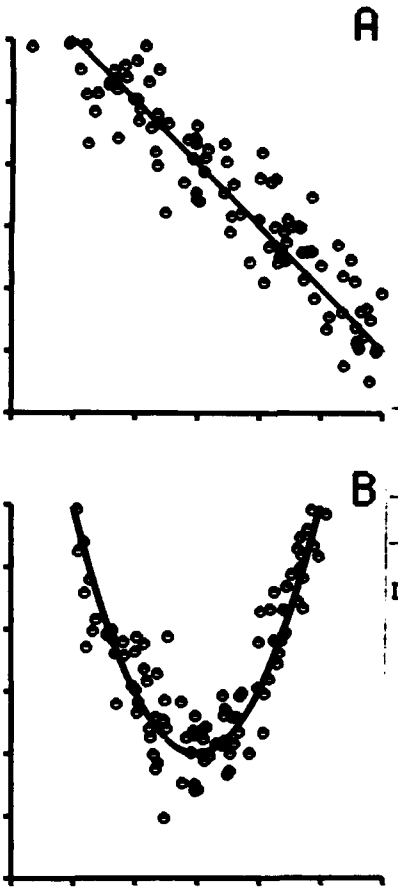

Figure 2. Two-dimensional analogs to the three-dimensional data systems to which trend surface analysis is applied. A) A linear regression line is fit to data that plot in x–y coordinate space as an elongate cloud. The regression line is fit using least-squares minimization of the total variance in the system. B) A quadratic equation is used to fit data that plot nonlinearly.

and the scale of variation in the data that is modeled. Equations with terms of increasing order describe features of successively finer scale and greater complexity. A first-order polynomial equation defines a surface that is a flat plane, with slope inclined in the direction of the mean intensity gradient across the image. The second-order surface combines this plane with a surface having a single flexure. The third order surface adds flexure in two directions, and so on. As in the two-dimensional case, a best fit is achieved by adjusting coefficients of the polynomial equations.

The general form of trend surface equations is shown here using the fourth-order equation (so called because it includes terms with variables raised as high as the fourth power) as an example:

$$\begin{aligned} Z_4 = {} & b_0 + b_1{*}x + b_2{*}y \\ & + b_3{*}x^2 + b_4{*}x{*}y + b_5{*}y^2 \\ & + b_6{*}x^3 + b_7{*}x^2{*}y + b_8{*}x{*}y^2 + b_9{*}y^3 \\ & + b_{10}{*}x^4 + b_{11}{*}x^3{*}y + b_{12}{*}x^2{*}y^2 \\ & + b_{13}{*}x{*}y^3 + b_{14}{*}y^4, \end{aligned} \tag{1}$$

where the b_i are the trend coefficients defined in the analysis and Z_4 is the height of the fourth-order trend surface associated with image location (x, y). Trend equations of lesser order are subsets of Eq. (1); equations of higher order add terms that follow the pattern of coefficients and exponents shown above. Trend coefficients (b_i) are derived by solving a series of simultaneous equations defined by substituting the sequence of pixel values in the original image and best-fitting the two-dimensional linear regression surface to these equations using the least-squares criterion described previously. As is evident from Eq. (1), calculation of higher order surfaces involves reduction of matrices of monotonically increasing size.

Once the series of desired polynomial surfaces Z_n is defined, the original surface (here an image) can be decomposed into components of regional and local interest. Specific polynomial surfaces can be removed from the original surface defined by the raw data by subtracting the mathematical trend surface from the original surface, thereby creating a residual surface. For example, the regional slope or dip of a surface can be removed by subtracting the surface defined by the best-fit first-order polynomial surface.

In the application reported here we seek to separate broad, region-scale trends in radiance that represent variation in illumination, surface temperature, or cloud cover from smaller-scale, higher-frequency features observed in the polar ice packs such as leads, fractures, ice floes, and changes in ice type. In a symbolic sense, if the regional and local components of the image are defined as R and L, then

$$I = R + L, \tag{2}$$

where I is the original image and R and L each are some combination of trend surfaces Z_n. The image we seek to produce, which is the image that contains only the local trends, then, is defined by

$$L = I - R, \tag{3}$$

and is obtained by subtracting trend surfaces that carry the region-scale information from the radiances in the original image. In the present study, we have added a constant C to the image such that

$$L + C = I - R + C, \tag{4}$$

where C is related to the mean z-value of the image. The purpose of C is to eliminate negative intensity values in the detrended image and to create a scene that consists of values that fall within the same range as values in the original scene. As such, the value assigned to C, although somewhat arbitrary, typically is the absolute value of the smallest negative radiance in the detrended scene.

APPLICABILITY OF THE TECHNIQUE

Trend surface analysis is applicable to data consisting of a coordinate position (x, y) and a measured value (z) that represents the height of the surface at that point. In the current application, the surface is defined by image radiances (z coordinates) that are mapped in a matrix row–column coordinate system (x and y coordinates) as a series of pixels that form an image. As with standard regression techniques, we assume that we know the geographic coordinate (x, y) without error, and that the only significant statistical error is associated with z. Images in general satisfy this requirement. Although error in the location of the image swath on the ground can be significant due to poor ephemeris data or to uncertainty in the pointing direction of the sensor platform [see, e.g., Poe and Conway (1990)], the relative position

of one pixel with respect to another remains constant for all practical purposes. The x–y location of each pixel, measured with respect to the image frame of reference, thus is known quite well.

We also assume that the regional trend can be described by a linear function of some combination of the geographical coordinates x and y, and that the relationship defining the regional trend can be defined by a polynomial function between any two adjacent pixels. Images characterized by sharp discontinuities or other features not well described by polynomial functions thus are inappropriate to this type of analysis.

A third assumption is that the optimal criterion to use to define the ideal nth-order trend surface involves minimizing the squared deviations of local fluctuations from the trend in the z direction. This is a standard assumption for any regression technique. Results we present in subsequent sections suggest that, although the least squares criterion produces acceptable solutions in this application, alternative criteria that incorporate principles of fuzzy set theory may be more appropriate. This prospect is addressed in the Discussion section.

Finally, with regard to the current application, we assume that there exists a criterion for determining the order of the surface that provides optimum enhancement of the binary image. Several statistical tests have been employed by other researchers in other applications. Most of these tests assume the usual conditions associated with regression analysis, such as homoscedasticity for constant variance and heteroscedasticity for changing variance. Rarely will these conditions hold for this and similar applications that concern image data. The nature of AVHRR images suggests that, although there are relatively high degrees of autocorrelation among groups of adjacent pixels, this autocorrelation varies nonuniformly across the image. Without this pattern of autocorrelation, features such as fractures could not be detected. Criteria that can be used to identify optimum surfaces in the present context are discussed in a later section.

METHODOLOGY

The trend surface technique was applied to three AVHRR images to assess the effectiveness of the method in removing radiometric bias that contributes to regional variation in scene intensity. For channels that fall in the visible band (Channels 1 and 2), such bias most commonly arises from uneven illumination due to proximity of the scene to the terminator or to changes in sun angle across the scene. At high latitudes where the sun angle is low, slight changes in angle produce significant changes in illumination. Bias in channels that fall within the infrared band (Channels 3 and 4) arises from variation in the regional surface temperature field.

Clouds represent a secondary source of bias in both visible- and infrared-band images. Although test images used were selected for their low cloud cover, they were not cloud-free. In the absence of effective cloud-screening methods that consistently discriminate clouds from ice, however, none of the images was processed to remove clouds. Inasmuch as an operational application of the trend surface technique would run on images in which clouds would be present, clouds were not masked from the test images in order to assess robustness of the method with respect to moderate cloud contamination.

Image 1 (Fig. 3), which shows sea ice in the Lincoln Sea, was acquired on Channel 4 (10.3–11.3 μm, infrared) at 1553 Z on 18 March 1990. Images 2 and 3 (Figs. 4 and 5), which are coincident, show sea ice in the Beaufort–Chukchi Sea region and were acquired simultaneously on Channels 4 (Fig. 4) and 2 (0.725–1.1 μm, visible) (Fig. 5) at 2255 Z on 16 March 1989. All three images are 512 × 512 pixel subsections of larger full-resolution AVHRR local area coverage (LAC) images. Image 1 was constructed by sampling every pixel in every row within a 512 × 512 pixel area and shows AVHRR LAC data at full resolution. Images 2 and 3 were constructed by sampling every other pixel on every other line within a 1024 × 1024 pixel area and thus show data at half resolution. This second AVHRR image was subsampled to increase illumination bias in the Channel 2 image (Image 3, Fig. 5) by including a larger area within the scene.

An AT-compatible personal computer operating at an effective clock rate of approximately 13 MHz was used for all calculations. The present implementation computes trend surfaces using a subset of points derived from the raw image. A coarse image 32 × 32 values in size is created by averaging pixels in adjacent 16-pixel-square neighborhoods across each 512 × 512 pixel test

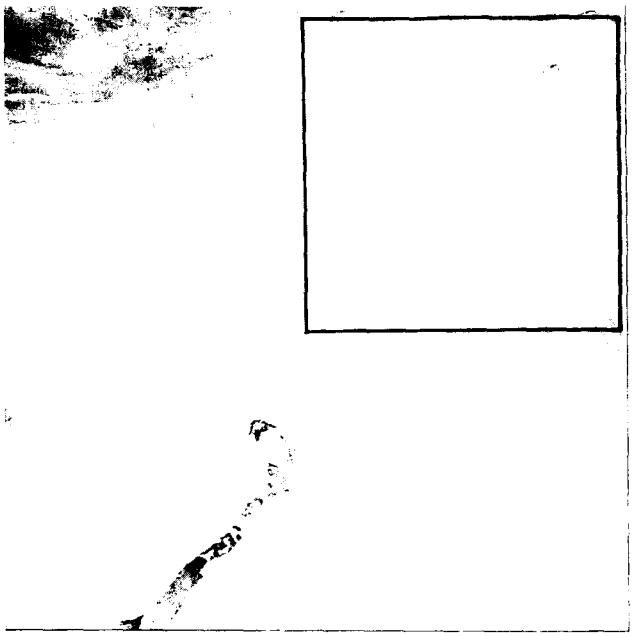

Figure 3. AVHRR Channel 4 scene used for Test Image 1 (Fig. 6). The image was acquired at 1553 Z on 18 March 1990 and shows sea ice north of Greenland and Ellesmere Island. North is at the top of the image. The Lincoln Sea and Nares Strait, which separates Greenland and Ellesmere Island, appear in the lower half of the image. Clouds obscure the upper left corner of the image. Image radiances have been inverted so that thermally cold thick ice appears white or light grey, and thermally warm thin ice in leads and in the polynya at the head of Nares Strait appears dark grey or black. Box at upper right indicates section of image used in this analysis.

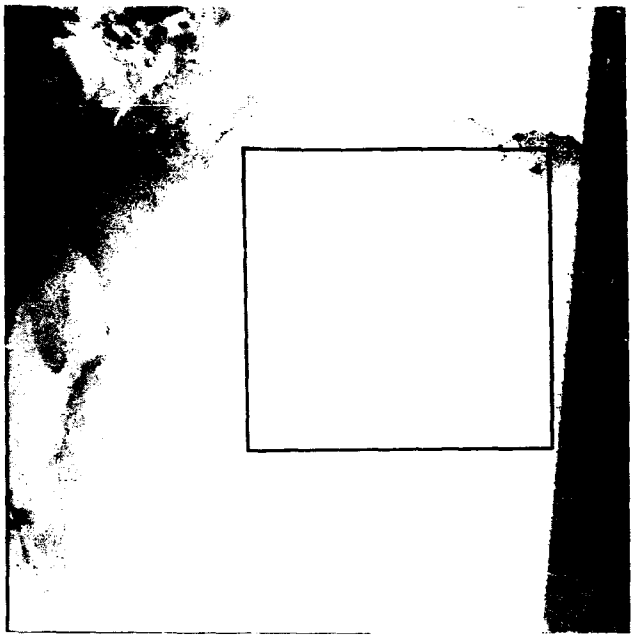

Figure 4. AVHRR Channel 4 (infrared) scene used for Test Image 2 (Fig. 7). The image was acquired at 2255 Z on 16 March 1989 and shows ice in the Beaufort, Chukchi, and East Siberian Seas. North is at the lower right corner of the image. The Alaskan coast appears at the middle left edge, the Chukchi Peninsula (Russia) appears in the upper left corner (partially shrouded in clouds), and the coast of Siberia appears along the upper edge. The box marks the section of the image used in this study. This area was sampled at half resolution by taking every other pixel in every other row. Wrangel Island is just outside the upper left corner of the box. The Anjou Islands (from left to right Ostrov Novaya Sibir', Ostrov Faddeyevskiy, and the east part of Ostrov Kotel'nyy) appear above the right corner of the box. Zhokhova and Bennett Islands are visible within the upper right corner of the box. The entire scene shown here is 2048 × 2048 pixels in size. Image radiances have been inverted so that thermally cold thick ice appears white or light grey, and thermally warm thin ice in leads appears dark grey or black.

image. (Use of neighborhoods of different size and application of different weighting functions that account for distance from the cell center currently are being explored. These results will be reported in a subsequent article.) The polynomial coefficients [b_i, Eq. (1)], which are derived from this smaller scene are used to construct a larger trend surface 512 × 512 pixels in size that is then subtracted from the raw scene. Use of a 32-pixel-square scene satisfies Nyquist sampling limits for a sixth-order trend surface, the highest-order surface that we compute.

Derivation of trend surface coefficients (b_i) from this smaller image rather than from the full scene holds two advantages. First, use of mean values derived from small areas of the image subdues pixel-to-pixel effects of local features such as leads and fractures that occur with high spatial frequency. Use of the coarse image has two advantages in this regard. First, although we wish to preserve lead and fracture signatures in processed images (after all, enhancement of these features is the objective of this exercise), we seek to limit the influence they exert on the shape of trend surfaces that are computed. Their presence could violate the second assumption that underlies the trend surface method (discussed above) which requires that gradients within small neighborhoods be gradual rather than steplike so that they can be described accurately by a polynomial function. Second, the coarse 32 × 32 pixel image captures regional trends in radiance that occur with low spatial frequency that we want to remove. Trend surfaces that are computed from this reduced image thus are less likely to be affected

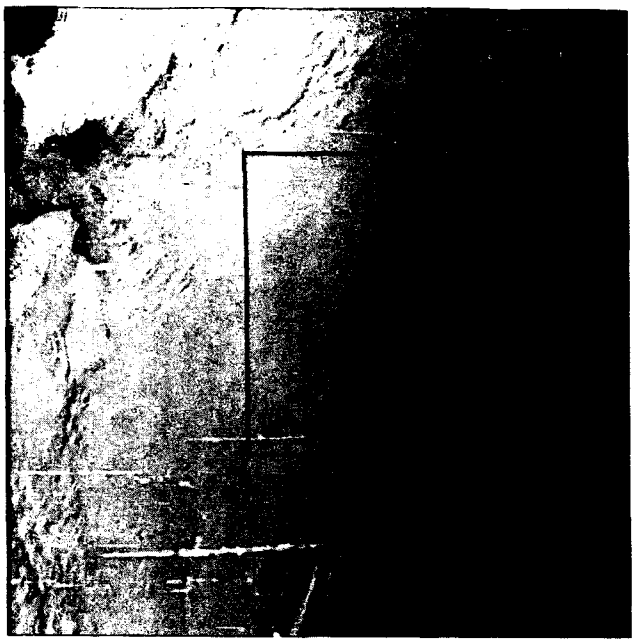

Figure 5. AVHRR Channel 2 (visible) scene used for Test Image 3 (Fig. 8). The image is the Channel 2 counterpart of Test Image 2 (Figs. 4 and 7) and shows the same geographic area. Refer to the Figure 4 caption for details.

significantly by local aberrations in radiance than had all pixels in the scene been used.

Second, computation time and programming complexity are reduced significantly by using the 32 × 32 pixel subset of points, thereby making use of AT-compatible personal computers feasible. Because of the small, fixed size of the coarse image, acceleration techniques can be applied easily to reduce both execution speed and memory requirements by significant margins. The result is that even in the slow computing environment offered by AT architecture results were obtained relatively quickly. Processing time ranged from approximately 30 s to produce a first-order surface of a 512 × 512 pixel image, to approximately 6 min for the sixth-order surface. From Eq. (1), we expect processing time required to compute higher-order surfaces to increase monotonically as a function of polynomial order.

Each of the three test images was processed in raw form without prior application of transforms, edge enhancements, or filters that traditionally are used to improve definition of leads. First-order through sixth-order trend surfaces were computed first. Then trends defined by each surface were removed from the original image simply by subtracting values of each successive trend surface from values in the original image on a pixel-by-pixel basis according to Eq. (4). Finally, a binary segmentation was performed on each detrended scene to determine visually whether lead definition was improved by the procedure.

Binary segmentation is a function which classifies each pixel as either a lead or not a lead based on its intensity (z coordinate) with respect to some threshold value. If the pixel is classified as a lead, the algorithm sets its value to 0 (black in the image). Otherwise its value is set to 255 (white) (Fig. 1). The threshold intensity used to segment each test image and its family of detrended images was chosen subjectively (on the basis of visual analysis of segmented images) to provide good lead definition in the detrended products: Too high a threshold produced an abundance of discontinuous lead segments and isolated lead pixels; too low a threshold produced broad, thick leads and misclassified low-radiance pixels in background ice as lead pixels. Different threshold values were chosen for each of the three test images, but the same value was used for all detrended scenes derived from a particular test image.

RESULTS

Figures 6, 7, and 8 show results of the trend surface analysis. Each figure consists of seven rows of images, one for the original image and one for each of the six trend surfaces of orders one through six. Each row includes three images: the trend surface on the left, the detrended image in the middle, and the binary segmentation of the detrended image on the right.

For display purposes raw grey levels in trend surface images (left column, Figs. 6, 7, and 8), which span a range of approximately 50 radiance units, have been stretched to enhance contrast using a minimum–maximum range transformation. Pixel intensities in the stretched images, although they fall across a range of 256 intensity levels, still only occupy approximately 50 discrete grey levels. As a result, the trend surface images take on a banded appearance that portrays contours of the trend surface well. The number of grey levels that are present in a given trend surface image is equivalent to the range of values represented by the surface. The width of a grey

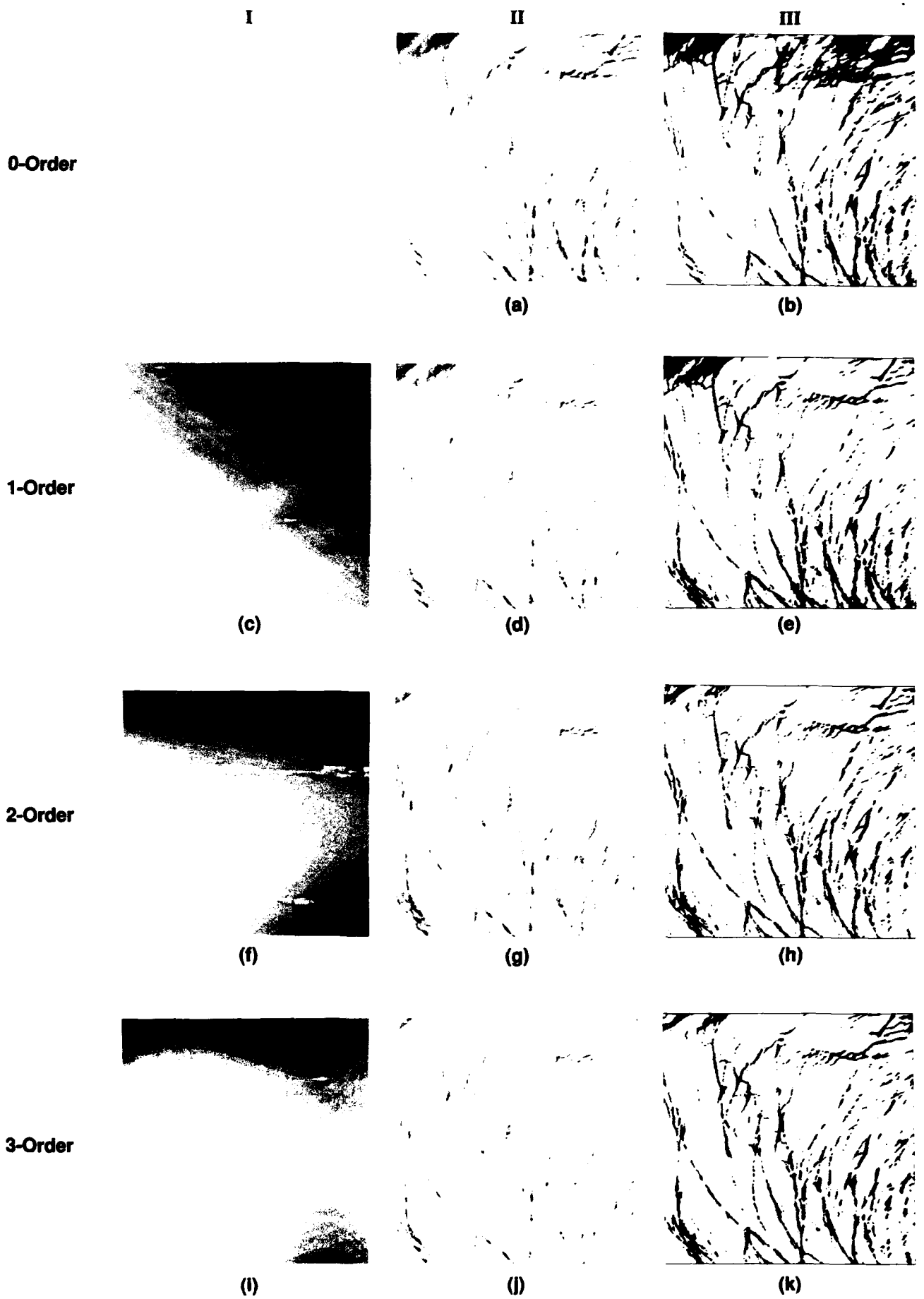

Figure 6.

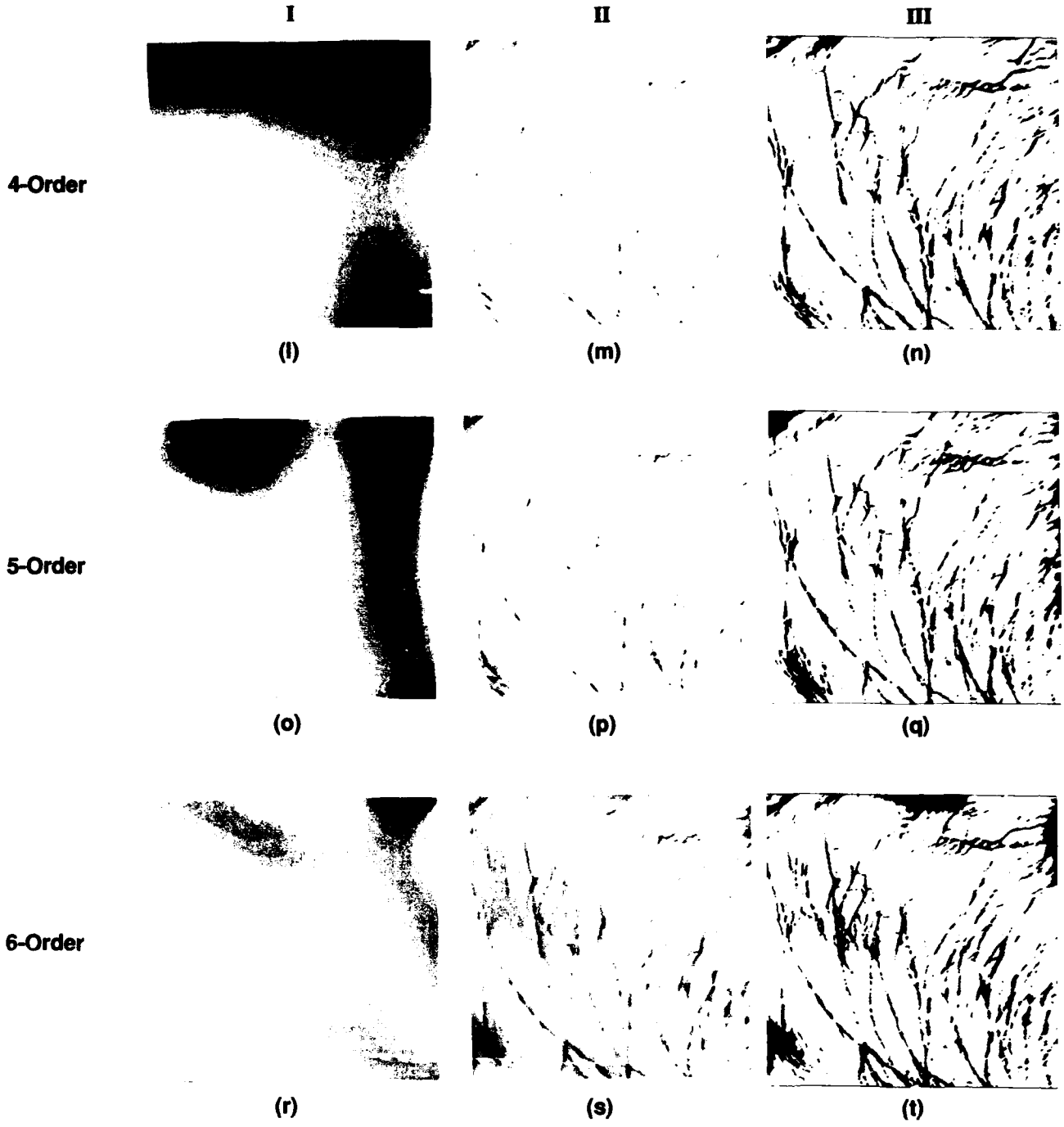

Figure 6. Trend surface analysis of the 512 × 512 pixel subsection of the Channel 4 AVHRR scene outlined in Figure 3. The processed scene was constructed by sampling every pixel in every row of the subsection area of the original image and so shows lead features at full spatial resolution. Processed images are arrayed in three columns and seven rows. Images in the first column show the topography of the trend surface that was removed from the original image, images in the second column show the image after the trend surface has been removed, and images in the third column show the image that results when a binary segmentation is applied to the detrended scene. Images in the first row show the raw unprocessed scene, images in the second row the result of removing the first-order surface, images in the third row the second-order surface, and so on up to the seventh row which shows the effect of removing the sixth-order surface.

step is proportional to the slope of the surface. Dark tones mark low points on the surface and light tones highpoints. Note that the complexity of the surface increases with increasing polynomial order from a simple sloped plane (first-order surface) to successively more complex surfaces which, in some instances, include convolutions that form hills and valleys (see especially Fig. 7, sixth-order surface).

Image 1 (Fig. 6)

Removal of the first- through third-order surfaces results in improved uniformity of grey tones

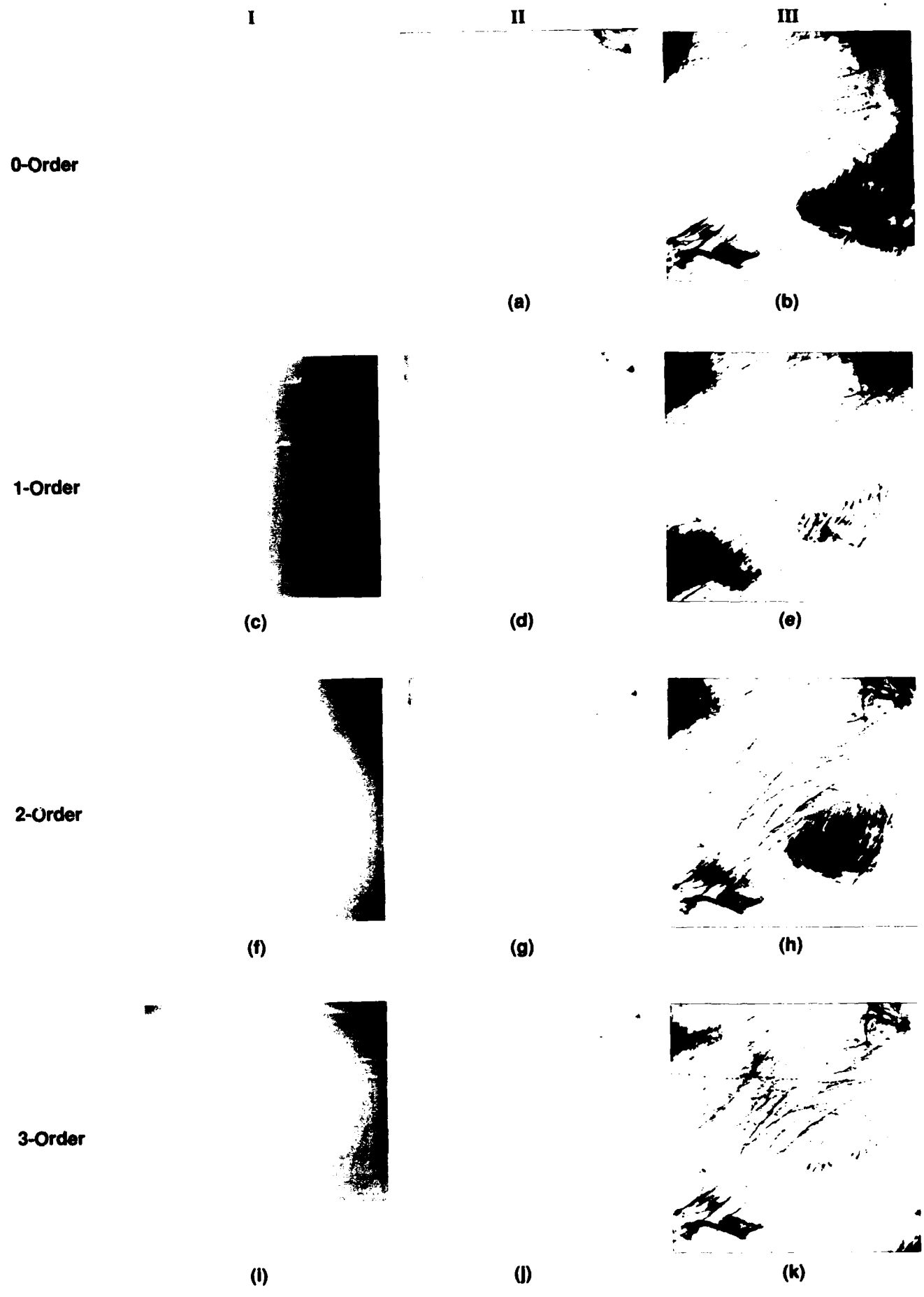

Figure 7.

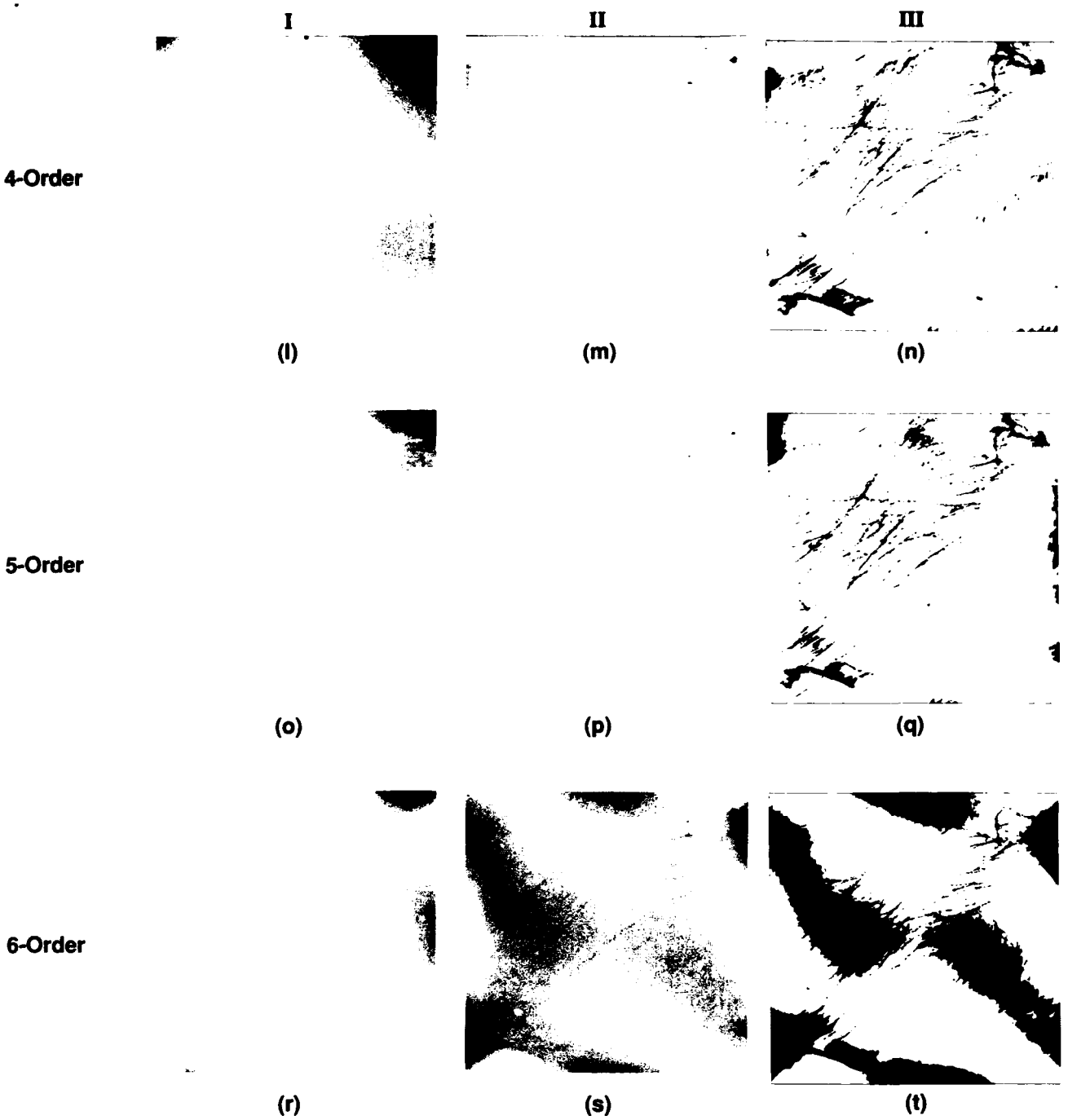

Figure 7. Trend surface analysis of a 512 × 512 pixel subsection of the Channel 4 (infrared) AVHRR scene shown in Figure 4. The processed scene was constructed by sampling every other pixel in every other row from the original image and so shows lead features at half-resolution. See caption to Figure 6 for description of images shown here.

across the detrended image (middle column, Fig. 6). Note especially the lighter tones evident with subtraction of each successive surface in the upper left corner and, to a lesser extent, along the upper border and lower right border. Significant visual differences are not evident between the third- and fourth-order images; indeed, the third- and fourth-order trend surfaces appear to be nearly identical. Such is not the case, however, when the fifth- and especially the sixth-order surfaces are subtracted. Artifacts related to the less than optimum fit (optimum in a visual sense) between the trend surface and broad-scale variation in radiance appear as alternating dark and light zones that trend diagonally across the detrended image from upper left to lower right.

Segmentation of the original image (first row, middle column, Fig. 6) overemphasizes leads along the upper border and, to a lesser extent, in the lower right quarter of the image. Leads along

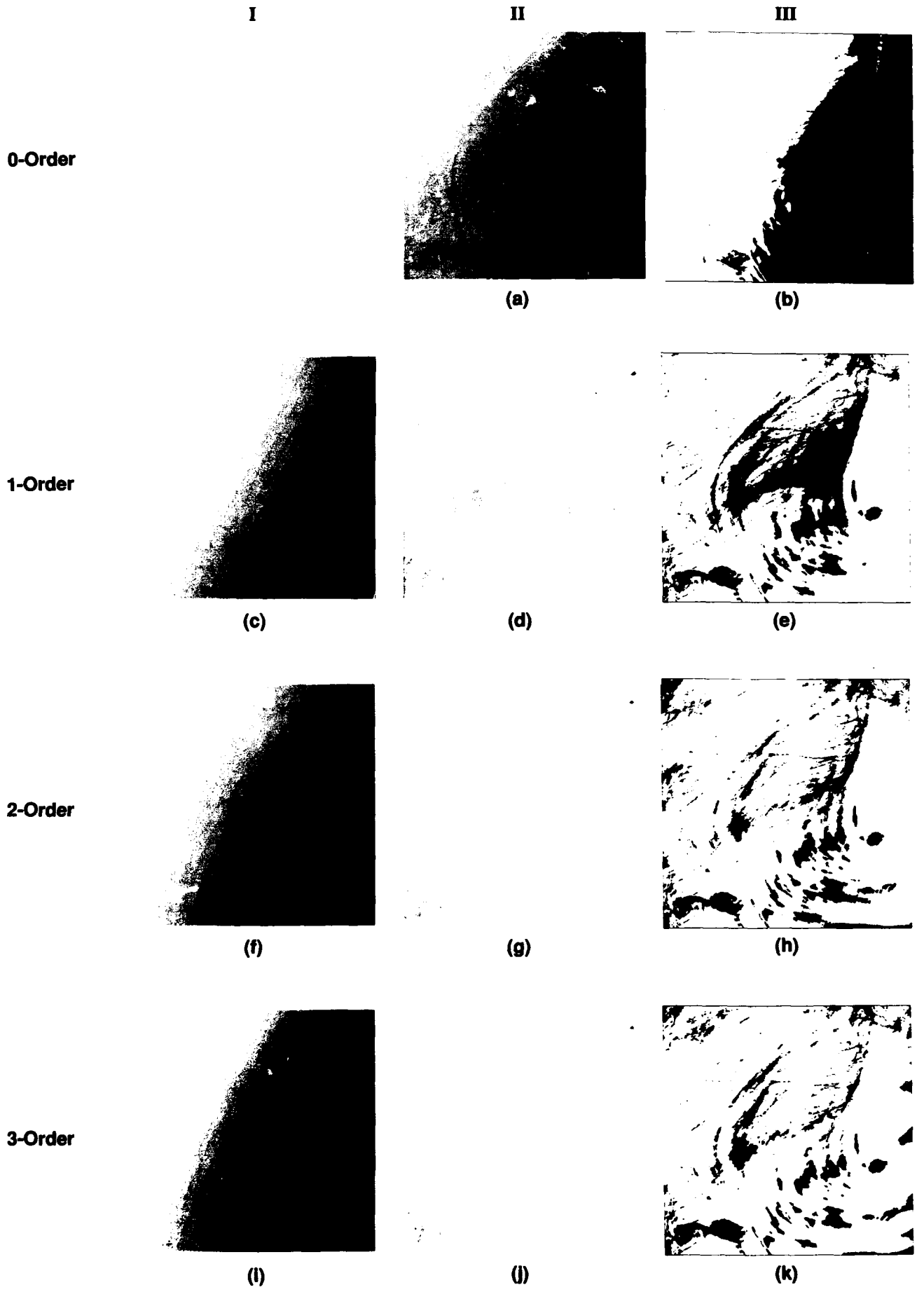

Figure 8.

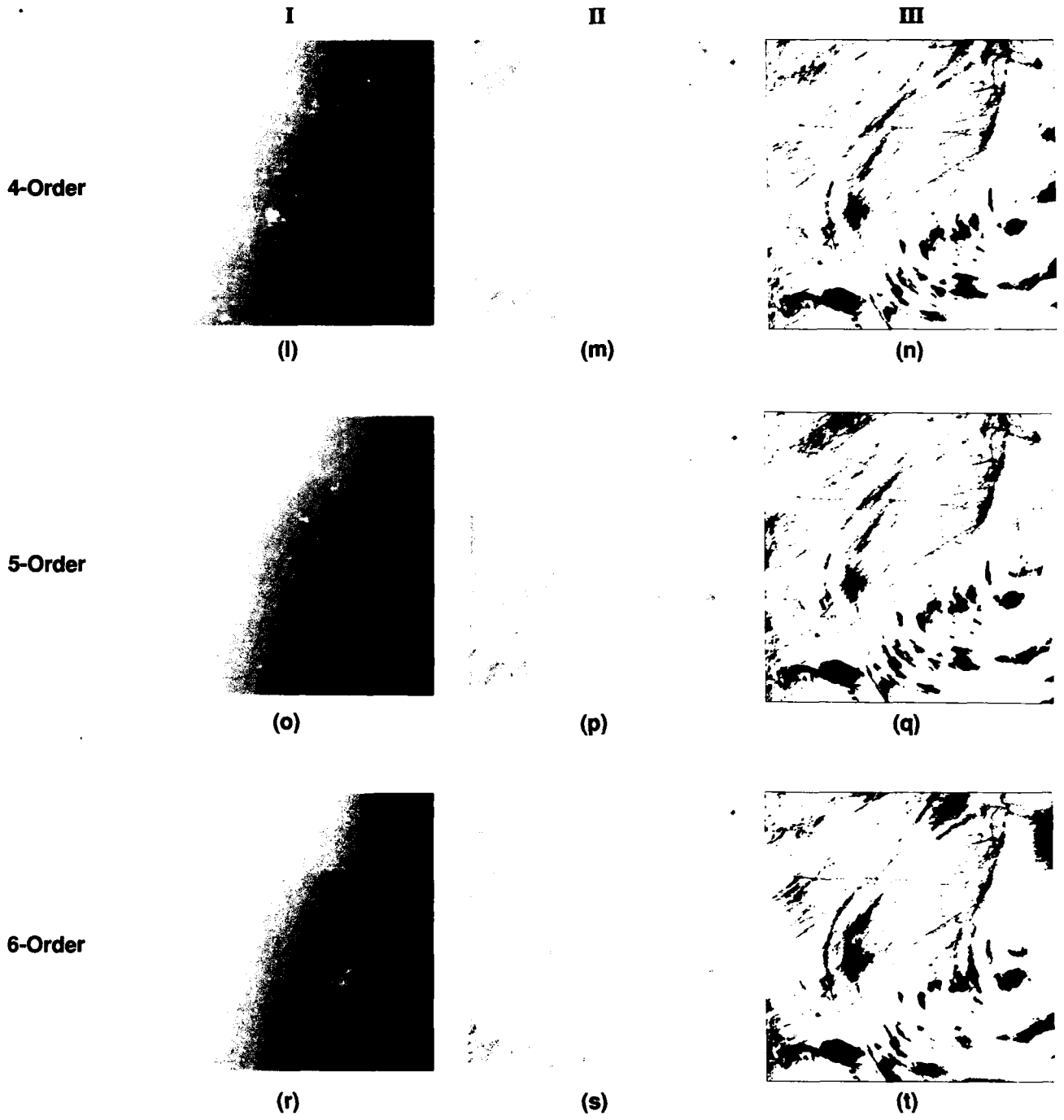

Figure 8. Trend surface analysis of a 512 × 512 pixel subsection of the Channel 2 (visible) AVHRR scene shown in Figure 5. The processed scene was constructed by sampling every other pixel in every other row from the original image and so shows lead features at half spatial resolution. Refer to the caption for Figure 6 for further description of images shown here.

the left edge and in the lower left quarter of the image, on the other hand, generally are underemphasized as evidenced by their discontinuous character. Removal of the first-, second-, and third-order surfaces improves the appearance of leads in segmented images significantly. Lead width is more uniform and the continuity of lead elements generally is improved, particularly in the second- and third-order segmented images.

Subtraction of the fourth-order surface yields no significant visual improvement over the third-order segmented image, and subtraction of the fifth- and sixth-order surfaces actually degrades visually the quality of the segmented image considerably. Neither of these higher-order surfaces (fifth- and sixth-order) approximates broad-scale changes in radiance that we are trying to correct particularly well. As a result, they overcorrect for broad-scale trends, decreasing the radiance in some areas and increasing it in others. This forces

the width and continuity of leads observed in binary segmented images to vary from region to region.

Image 2 (Fig. 7)

The signature of clouds, which partially obscure the surface in the right half of Image 2, produces image radiances that are close in value to radiances typical of leads. When the raw image is segmented (Fig. 1 and Fig. 7 top row) clouds are classified as leads. Lead patterns in the segmented image thus either are totally obscured in the vicinity of clouds (solid black areas) or at best are confounded by cloud bands (feathery patterns at edge of solid black areas).

Removal of the first- through fourth-order trend surfaces results in progressive improvement in lead definition in both the detrended image and the segmented image. Cloud signatures are subdued, which is particularly evident in the segmented image, and the overall tone of the detrended image becomes more uniform. Lead traces in both the segmented image and the detrended image become clearer, especially when the third- and fourth-order surfaces have been subtracted. Clouds, where they are thickest in the lower right quarter of the image, continue to obscure most leads, as the low number of lead traces observed in the segmented images suggests.

The image is not improved by removing trend surfaces of higher order (fifth- and sixth-order). Although subtraction of the fifth-order surface darkens lead traces in the central portion of the segmented image and makes them appear to be more continuous, spurious pixels that probably do not correspond to well-defined leads also are highlighted (most notably at top center). These pixels are likely to complicate subsequent efforts to locate leads using automated methods (Fetterer and Holyer, 1989). Moreover, effects of clouds that previously had been eliminated along the right margin and in the upper left corner of the image have reappeared. The feature at lower left, which probably is a frozen polynya, lacks definition that was present in the previous binary images (second through fourth order).

Removing the sixth-order surface leads to a totally unacceptable result. The detrended image takes on a blotchy appearance. Broad patterns that have no apparent relationship to the array of leads that is present in the scene appear in the segmented image. Alternating dark and light zones are offset across a line that runs diagonally across the binary image. This result clearly lacks utility, although from a mathematical perspective the result is valid insofar as the trend surface both represents the best-fit sixth-order polynomial to the surface defined by the raw image radiances and accounts for the greatest amount of variance in the scene on the basis of the least-squares criterion. In this case, however, the raw image lacks features that recur at spatial frequencies that a sixth-order equation approximates well. This illustrates in graphic fashion one of the potential pitfalls of using trend surface blindly without assessing the validity of the solution in some way, whether by visual or automated means.

Image 3 (Fig. 8)

The third test image is coincident with the second, but was acquired at visible frequencies (Channel 2) rather than in the infrared band (Channel 4) as were Images 1 and 2. The dominant bias that must be removed from visible band images for successful lead segmentation arises from uneven illumination rather than from thermal variation. Clouds, which constitute a secondary bias in Channel 2 data, affect analysis of visible images to a greater extent than infrared images because the opacity of clouds is greater at visible frequencies.

Image 3 shows clearly the effect of uneven illumination caused by changes in sun angle across the scene. The raw image darkens progressively toward the lower right corner in the direction of the terminator (Fig. 8, first row). Effects of this falloff in radiance dominate the segmented image, which is essentially half white and half black. Leads are evident along a narrow band that parallels the margin of the black area, but they become increasingly discontinuous with distance away from the margin.

Subtraction of the first-order trend surface from the raw image produces significant improvement (Fig. 8, second row). Bias caused by illumination is effectively removed. The detrended scene appears to be lighted uniformly; progressive darkening toward the lower right corner of the image is not evident. The corresponding seg-

mented image shows leads distributed more uniformly across the scene, but bias caused by clouds continues to obscure lead trends, particularly in the central region of the image.

Removal of the second-, third-, and fourth-order trend surfaces reduces cloud bias significantly. Although isolated, black patches remain in the segmented image where higher cloud tops cast shadows on the ice surface, lead trends for the most part are continuous and can be followed across the scene. Removal of the fifth-order surface produces slight enhancement in leads along the right border of the segmented image, but degrades lead definition along the left border. Application of the sixth-order surface results in overall enhancement of cloud features at the expense of lead signatures. As a result, lead traces are suppressed in some areas and overly enhanced in others.

DISCUSSION

These results suggest that application of polynomial trend surface analysis to raw AVHRR images improves definition of leads when binary segmentation procedures are applied subsequently. Lead traces are more uniform in character, show fewer discontinuities and changes in width, and extend across longer distances in binary images derived from detrended scenes. In each of the three test images, optimum results, as judged visually by these criteria, were obtained by removing trends defined by the fourth-order surface (Figs. 6, 7, and 8).

Subtraction of the first- and second-order trend surfaces removes broad-scale, regional trends in radiance, but these orders alone are insufficient to describe variation in radiances on smaller spatial scales typical of cloud patterns. Subtraction of the third-order surface produces substantial improvement in lead definition in the segmented image where thin clouds are present. Confusion between lead trends and cloud structures generally are not resolved fully, however, unless the fourth-order trend surface also is applied. Even then, some ambiguities remain. In all cases higher-order trends, represented by fifth- and sixth-order polynomials, fit broad-scale variation in image radiances poorly, obscure lead trends in segmented images and make lead identification more difficult. This despite the fact that these higher-order surfaces represent a better mathematical and statistical estimate of total variance present in the image.

Specific test images that were used were selected both because they show well-developed lead signatures and because they are relatively cloud-free. This bias undoubtedly affects the outcome of the analysis and leaves open questions concerning general applicability of the method to more typical AVHRR images in which clouds dominate, lead trends are less distinct, and lead width and density varies significantly across the scene. In assessing the applicability of trend surface methods to operational use of AVHRR data in general, two points in particular become important. The first point concerns selection of the optimum polynomial order to apply. The second point concerns applicability of the technique to images in which clouds dominate or in which lead density varies erratically across the scene.

What is the Optimum Polynomial Order to Apply?

The manner in which the optimum polynomial order that best describes region-scale variation in illumination or temperature is determined is somewhat subjective, which presents problems if the trend analysis technique is to be implemented in an operational environment. Stated differently from an operational perspective, how does an analyst arrive at the correct polynomial order, the order that produces optimum lead definition? Further, how typical are the solutions derived here in which low-order surfaces capture regional bias due to illumination and intermediate-order surfaces capture local effects of clouds?

For the Channel 2 scene analyzed here (Fig. 8), the first- and second-order trend surfaces effectively remove broad-scale effects of variable illumination. We expect that these low-order surfaces will be equally effective when applied to most AVHRR Channel 1 and Channel 2 scenes. Illumination intensity is a function of both the earth's curvature, which determines the angle at which sunlight impinges on the earth's surface, and, indirectly, the thickness of atmosphere through which sunlight must pass to reach the surface. Although the magnitude of observed deviations in illumination increases with distance

across a scene, the curvature and slope of surfaces that describe these trends is anticipated to remain relatively constant, at least across distances typical of AVHRR images. Change in season may alter spatial characteristics of the effect of illumination somewhat, but such temporal changes should repeat annually in a predictable manner as the seasonal cycle progresses. In general, then, the first- and second-order trend surfaces can be expected to capture broad-scale variability in radiance attributed to illumination with a high degree of consistency. The trend surface technique thus represents an alternative to conventional methods that use orbital elements and scene geometry to correct for illumination bias.

Low-order trend surfaces also capture variability in Channel 4 radiances that probably is related to region-scale variation in the surface temperature field. Modest improvement observed in segmented versions of Figures 6 and 7 from which the first-order surface has been removed supports this contention. Surface temperature is not as well behaved as illumination, however, and spatially dependent temperature effects that occur at higher spatial frequencies will not be removed completely by low-order surfaces. Anomalies that mark local departures from the regional temperature trend thus will persist in the segmented product and must be removed using higher order surfaces. Nonetheless, application of the first- and second-order trend surfaces to Channel 3 and 4 images probably will lead to at least limited improvement in segmented scenes in most instances.

With the broad-scale trends of illumination and temperature removed, clouds and local temperature effects represent the dominant factors that limit clear definition of lead trends in the segmented product. For the three scenes analyzed here, the third- and especially the fourth-order trend surfaces consistently produce the most significant improvement. It is unclear, however, whether the third- and fourth-order surfaces represent the best descriptors of regional scene variability in other cases.

The appropriate polynomial order is functionally related to spatial variability of radiances across a scene and how that variability is distributed in a geographic sense. The fourth-order surface probably does a good job in images analyzed here because spatial variability typified by the fourth-order surface matches well the scale and pattern of variation shown by intermittent clouds. In scenes with cloud cover similar to that shown in the test images, then, we anticipate that removal of the fourth-order surface will yield significant if not optimum improvement.

Images in which clouds either cover a larger percentage of the scene or are arrayed in patterns that are described poorly by a fourth-order polynomial equation may not benefit significantly from removal of fourth-order trends. Test images used for this study were selected because they show well-defined lead patterns and because they are relatively cloud-free. As a consequence, they do not represent the range of cloud conditions typical of arctic AVHRR scenes. In some cases higher (or lower) order surfaces might capture unwanted trends more completely than the fourth-order surface that worked well here. Additional work is required to establish whether a systematic relationship exists between percent cloud cover, patterns in which clouds are arrayed, and the polynomial order that optimizes lead definition in segmented images.

Can the Method be Applied with Similar Results to All Scenes?

The trend surface technique yielded promising results when applied to the small number of scenes analyzed here. Questions remain concerning whether the method can be applied generically to images that show a range of different lead distributions and cloud characteristics and still produce uniform results. Couched in slightly different terms, how do *n*th-order detrended images compare when one image shows few leads, another shows a large number of leads evenly distributed across the scene, and a third shows an intermediate number clumped in an uneven pattern? The question is equally valid with respect to effects of variable cloud distribution.

Lead Distribution

The morphology of higher-order polynomial surfaces is defined by the mean radiance of the image over increasingly shorter scales. Variation in local image intensity assumes greater influence over the shape of the surface with increasing polynomial order. The dominant factor affecting image intensity at these smaller scales is the percent of

the surface area that consists of leads or, in the case of highly obscured images, clouds. We speculate that trends expressed in fifth- and sixth-order surfaces in images that are relatively cloud-free may be related in some instances to local lead density and width, both of which contribute to variation in mean radiance measured over intermediate distances.

According to this model, valleys in higher-order trend surfaces mark sites in which leads cover a large fraction of the surface and peaks mark sites in which few leads occur. Trends so defined by higher-order polynomials thus may map, at least to some extent, regional patterns in lead density and width. Qualitative (visual) comparison between lead density and the sixth-order trend surface computed for Figure 7 suggests such a relationship. Although this in itself may be useful information in some applications, it is not necessarily a desirable effect where optimum lead enhancement is the goal, particularly if lower-order surfaces used to remove trends in illumination and surface temperature are also corrupted by variation in lead density. This raises questions concerning the degree to which similar information is partitioned in the same order surface when the underlying scenes differ significantly in character.

Although a rigorous test of the effects of scene character on trend surface results is beyond the scope of this paper, the current work suggests that effects of differences between source images can be minimized in two ways: by modifying the conventional least-squares criterion used to define polynomial coefficients that produce the best-fit surface, and by careful selection of values that comprise the coarse 32 × 32 pixel image from which trend surfaces are derived. This work is being pursued, and we outline the approach being taken.

Alternatives to the least-squares criterion: The trend surface technique applied here uses a conventional least-squares criterion to determine the best-fit surface to the image data. In statistical parlance, the least squares criterion is a strict variance technique. That is to say, the fit is based on the least-squares minimization of the total variance in the data. In practice, the best-fit surface is found by minimizing the sum of squares of the distances from each of the data points (pixel values) in the image to the candidate trend surface.[1] Implicit in this conventional application of the least-squares method is the assumption that all pixels in the image are of equal importance and carry equal weight in determining the configuration of the trend surface. Although results presented here suggest that this method produces acceptable results, the equal weight assumption may not be optimum for the present application. This is especially true when scenes with uneven lead density are analyzed. Two hypothetical examples show why.

Figure 9A shows a regression line fit to a series of points plotted in an x–y coordinate system. Most of the data fall within an elongate cluster, but two points plot as outliers at a significant distance from the main data cloud. The regression line fit to all of the data passes through the central region of the main data cloud and generally follows its trend. However, the two outliers clearly influence the position of the regression line. It slopes more steeply than the general trend of the main data cluster, and it falls outside of the main cluster for large and small values of x and y. Figure 9B shows a case in which data are arrayed in two elongate clouds oriented along parallel trends. The regression line approximates the slope of the trend well but falls in a region between the two data clouds where no data are located. In both cases (Figs. 9A and 9B), the regression line summarizes some aspects of the data well, but on the whole it provides a distorted picture of the overall structure of the data.

AVHRR images present analogous situations to these two-dimensional examples. We seek to model the surface defined by radiances of the sea ice pack by computing the trend surface that best fits the data. Ideally most of the pixels in the image represent radiances of thick, mature pack ice (thick first-year ice and multiyear ice). Pixel values that correspond to leads lie above or below the surface that mature ice pixels define, depending on AVHRR channel. A best-fit criterion applied in the conventional least-squares sense gives equal weight to all pixels. The topography of the trend surface fit on this basis thus is at best shifted (Fig. 9B) and at worst warped (Fig. 9C) by the influence of lead pixels. Although the sur-

[1] Actually, as described above, a hybrid subset of points derived from the image is used here. This discussion is equally valid, however, whether the full set or a subset of points is used.

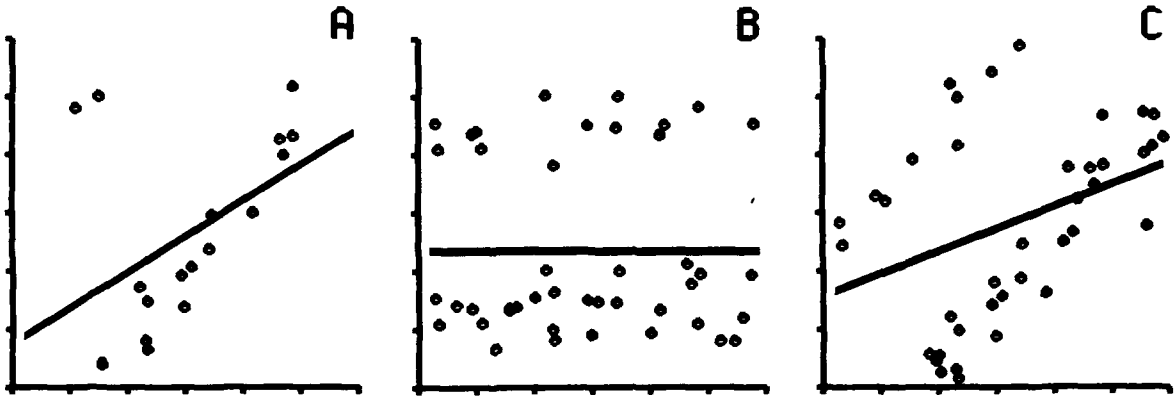

Figure 9. Two examples of data sets with structures described poorly by regression lines fit using a least-squares criterion. A) Two outliers at distance from the main data cloud contribute a disproportionate amount of variance to the system and deflect the regression line away from the primary data cloud. As a result, the regression line poorly represents the trend displayed by the bulk of the data. B) The data are arrayed in two separate clouds with parallel trends. The regression line represents the slope of the trend well, but falls in an area where no data occur. C) Introduction of a steep slope to the data structure complicates interpretation of the trend further.

face that is computed approximates trends in radiance of the mature ice surface, bias related to uneven illumination or to anomalies in the surface temperature field cannot be removed completely because the topography of the computed surface is confounded by secondary trends induced by lead pixels.

Images in which lead density is uniform across the scene probably are relatively unaffected by this problem. In such a case, the shape of the best-fit surface should conform well to trends in mature ice radiances, although it will be offset a constant distance toward values of lead pixels (Fig. 9B). However, lead density is unlikely to be uniform across AVHRR images. The shape of trend surfaces computed to estimate illumination or temperature fields for most images thus will be distorted to mimic patterns in lead density (Fig. 9C), particularly for mid- to high-order polynomial surfaces, which describe patterns of higher spatial frequency. Clouds compound the problem, not because their radiance is significantly different from that of the mature ice pack, but because they mask leads, sometimes over broad areas, and in effect create the appearance of nonuniform lead density. Detrended images derived from scenes with similar illumination and temperature fields but different lead and cloud characteristics thus are not strictly comparable because the best-fit criterion forces a slightly different solution in each case.

The influence of lead and cloud pixels can be minimized if we discard the rule that all pixels receive equal weight when the least-squares distance to the trend surface is computed. The objective here is to emphasize regions of the image over which background radiances of mature ice are dominant and to deemphasize the contribution of lead pixels. We suggest two strategies for assigning weights; the optimum solution to the problem may well incorporate elements of each.

The first method, which is somewhat subjective in nature, relies on the analyst to designate those regions of the image to be used to define the polynomial surface. This would be done interactively using a mouse or some other cursor control device to outline areas to accept. In effect, the weights within these areas would be set to 1.0, and weights in undesirable areas would be set to 0.0. The trend surface, though calculated using radiances only from these selected areas, would be applied to remove trends across the entire image. The adavantage of this scheme is that the operator can monitor the process in real time, reject untenable solutions, and accept solutions that produce the best binary images. The disadvantages are that it is subjective in nature, it is relatively slow, and it cannot be automated completely, at least within the context of the current state-of-the-art.

The second scheme invokes fuzzy set theory to adjust weights in an automated, predictable manner. Distances between each data point (pixel radiance) and the polynomial surface would be

evaluated using fuzzy exponent functions (Bezdek, 1981; Bezdek et al., 1981; 1984; Full et al., 1982). The resultant fuzzy distance measures could be applied to assign weights to data such that points located at distance from the central region of the data cluster would exercise limited influence over the shape of the surface. Additional statistics such as fuzzy membership functions could also be used. These methods, which are well established, minimize the effect of a relatively small number of observations that otherwise account for a disproportionate amount of the total variability present in a data set. Advantages of this scheme are that the relative importance of data is evaluated objectively according to a consistent set of rules that take into account all of the structural information contained in the image, and that the scheme can be fully automated in an expert system.

Derivation of the coarse 32 × 32 pixel surface: Effects of lead geometry can be minimized by careful selection of values that comprise the coarse 32 × 32 pixel surface from which polynomial coefficients are computed. One approach is to examine the frequency distribution of raw pixel intensities that occur within each 16 × 16 pixel cell used to derive the 32 × 32 pixel surface, truncate the distribution to remove the tail that includes lead pixels, and then use the mean value of remaining pixels to represent the radiance of the cell. The difficulty in using this approach lies in determining the threshold value used to truncate the distribution, particularly in Channel 1 and 2 images where illumination varies markedly across the scene. Alternatively, the value could be selected in a two-step procedure that first employs fuzzy membership statistics to discriminate lead pixels from mature ice pixels, and then uses fuzzy distance measures to weight nonlead pixels based on their distance (measured here in the x–y coordinate plane) from the center of the 16-pixel-square cell.

Cloud Characteristics

Results discussed above demonstrate that the trend surface procedure produces significant improvement in lead definition in segmented images, even in scenes with moderate cloud cover (Figs. 7 and 8). Nothing was done in the current application to minimize deleterious cloud effects; in a sense, this represents a worst case test of the procedure for cloud conditions that the test images show. Our results might be improved and lead segmentation further enhanced if cloud cover is taken into account. Two strategies in particular could be applied in this regard: a) Cloud regions could be masked so that surfaces are computed using only those parts of the image in which the ice surface is visible, and b) an improved radiometric model of regional and local variation [Eq. (2)] could be developed for areas masked by thin clouds that are not optically opaque.

Cloud mask: Efforts to devise algorithms to identify ice-covered regions that are obscured by clouds using AVHRR data have not met with success. Prospects for development of cloud masks based on automated recognition of cloud-covered areas thus are poor.[2] However, ongoing work associated with our lead characterization effort suggests that lead-rich areas might be identified based on the unique variance structure of pixel neighborhoods in which leads occur. Lead radiances are significantly different from those of surrounding ice. The variance of pixels in lead-free zones and in cloud-obscured zones thus is less than the variance of pixels in zones where leads occur. The variance within the 16 × 16 pixel neighborhood used to derive the coarse 32 × 32 pixel image from which the trend surface is derived thus carries information concerning the presence or absence of leads and forms the basis for a criterion for identifying regions of the image to include in the trend surface analysis. In effect, this allows one to generate the inverse of a cloud mask.

Improved radiometric model: The model used here to remove undesirable trends from an image is additive: We treat the image as the sum of regional- and local-scale trends in intensity [Eq. (2)]. We believe that this model is appropriate under most circumstances, inasmuch as effects of both illumination and the surface temperature field add to background intensities observed from space. However, thin cloud through which the ice surface can be seen present a different situation that the simple additive model fails to describe completely. Energy sensed by the satellite con-

[2] The manual, subjective method of identifying desirable regions of the image to include in the analysis, discussed in a previous paragraph on *Alternatives to the least-squares criterion*, though applicable in a research environment, is manpower-intensive and too time-consuming to implement in an operational processing scheme.

sists of two components: upwelling energy from the ice surface that passes through the cloud on its way to the sensor and downwelling energy that is reflected upward from the cloud top to the sensor. Energy reflected from cloud tops adds to energy upwelling from the surface. But energy passing upward through the cloud is attenuated through absorption and scattering by water vapor and cloud droplets according to some extinction coefficient κ. Attenuation is a multiplicative process and, in this case at least, it alters information we seek to enhance concerning the character of the underlying sea ice surface.

The radiative model for portions of images that include thin clouds thus is more accurately described by

$$I = R_\kappa(L_i + R_i) + R_c. \quad (5)$$

All variables here represent surfaces that can be displayed as images. I is, as before, the surface defined by intensities in the raw image [Eq. (2)], R_κ represents a surface that embodies regional trends in the attenuation characteristics of the cloud which vary on regional scales, L_i and R_i are local and regional components of intensity that emanate from sea ice beneath the cloud, and R_c is the surface that describes region-scale components of intensity arising solely from energy emitted by or reflected from the cloud. Rearranging terms, we define the image that represents the local component of intensity originating from the ice surface as

$$L_i = \frac{I - R_c - R_\kappa R_i}{R_\kappa}. \quad (6)$$

Implementation of this model, though it probably would improve results presented here, not only is beyond the scope of the current study but exceeds the current state-of-the-art as well. First, it requires that thin clouds be identified unambiguously in AVHRR images of sea ice. The problem of recognizing thick, optically opaque clouds has not yet been solved satisfactorily for images of the polar regions; thin cloud represent an even more difficult problem. Second, once the clouds are identified, solution of Eq. (6) requires that the attenuating characteristics of these clouds be known. It is not clear that this information can be derived from cloud signatures in AVHRR data.

SUMMARY AND CONCLUSIONS

Polynomial trend surface analysis was applied to three AVHRR images of the arctic sea ice pack. The objective of the study was to determine whether polynomial trend surface analysis can be applied effectively to AVHRR imagery to remove artifacts related to uneven illumination, regional changes in surface temperature, and intermittent cloud cover. These phenomena significantly limit definition of leads in binary images that are produced when conventional segmentation techniques are applied to AVHRR scenes. Accurate segmentation of leads from background ice is an important prerequisite to certain automated lead characterization procedures (Fetterer and Holyer, 1989).

Two of the scenes analyzed were Channel 4 (infrared) images (Figs. 3 and 4) and one was a Channel 2 (visible) image (Fig. 5). Polynomial surfaces were fit to these image data using first- through sixth-order equations. These surfaces, which embody mean variation in image intensity on regional scales, then were subtracted from the original images [Eq. (4)]. Detrended images that result were subjected to binary segmentation procedures that classify the pixels in the scene as either leads or mature pack ice. Results of this study, obtained through visual analysis of detrended images, lead to the following conclusions:

a. Trend surface techniques are effective in removing region-scale variation in image radiances that are related to uneven illumination, intermittent cloud cover, and variation in the surface temperature field (Figs. 6, 7, and 8).
b. The dominant effects of illumination in Channel 2 data, caused by variable sun angle and proximity of the scene to the terminator, are described well by the first- and second-order trend surfaces. Subtraction of these surfaces from the raw AVHRR image effectively removes illumination bias for purposes of binary segmentation applications (Fig. 8). The trend surface technique thus offers an alternative to more conventional methods of removing illumination bias when orbital parameters and crosstrack geometry are not known in sufficient detail.

Figure 10. Binary image of the scene shown in Figure 1 with the fourth-order polynomial trend surface subtracted from the raw image. Both binary images (Figs. 1 and 10) were produced by segmenting the same scene using the same digital intensity threshold. Continuity of lead features is significantly enhanced across the entire scene. Lead structures developed around Zhokova and Bennett Islands at upper right are now visible. Clouds, which appear as a dark mass along the right edge of Figure 1, generally are not evident in the detrended image, although a few wind streets remain at right center. Areas along the right margin of the image in which no leads occur probably represent areas in which thick clouds mask the surface. Application of the trend surface technique has enhanced lead definition significantly by improving the continuity of individual lead elements and by eliminating confounding effects of clouds.

c. Low-order surfaces also remove regional variation in the surface temperature field, which leads to improvement in binary images derived from Channel 4 data (Figs. 6 and 7).
d. Optimum results for both Channel 2 and Channel 4 data are achieved when the third- and fourth-order surfaces are subtracted to remove local temperature and illumination anomalies that occur in the vicinity of clouds (compare Figs. 1 and 10).
e. Application of higher-order surfaces fails to improve image quality and in most instances degrades the segmented image significantly.

Significant questions remain concerning the extent to which the technique is robust with respect to differences in lead density, cloud cover, and patterns in which clouds are distributed across different scenes. For example, there is some indication that the topography of higher-order surfaces (fifth- and sixth-order) in part maps regional variation in lead density (see sixth-order surface, Fig. 7). Ongoing work, to be reported in a subsequent paper, is directed at limiting these effects. Preliminary analysis suggests that the least-squares criterion, used by conventional trend surface routines to define the best-fit polynomial surface, does not produce optimum results in this application. A criterion that allows for data to be weighted based on their distance from the plane about which they cluster in three-dimensional space is more appropriate to the structure of AVHRR radiance data typical of images that show sea ice, clouds, and leads. Methods that incorporate a rule system based on fuzzy logic offer an alternative to the least-squares method and show promise in this regard.

AVHRR imagery used in this study was supplied by Florence M. Fetterer of the Remote Sensing Branch (Code 321), Naval Oceanographic and Atmospheric Research Laboratory (NOARL). W. E. F. received support under a Summer Faculty Research Fellowship awarded by the U.S. Navy-American Society for Engineering Education Fellowship Program through NOARL's Basic Research Management Office (Code 114), Halcyon E. Morris, head. All other aspects of this work were funded by NOARL under program element 0602435N, Budd B. Adams program manager. We gratefully acknowledge the support and assistance of these sponsors. We thank L. Dennis Farmer, Florence M. Fetterer, Ronald J. Holyer, and Albert W. Green for providing critical readings of an early draft and two anonymous reviewers whose comments led to significant improvement of the manuscript. Substantive conversations with Jeff Key clarified issues that concern radiative transfer models. This is NOARL Contribution No. JA:332:029:91.

REFERENCES

Bezdek, J. C. (1981), *Pattern Recognition with Fuzzy Objective Function Algorithm*, Plenum, New York, 256 pp.

Bezdek, J. C., Trivedi, M., Ehrlich, R., and Full, W. E. (1981), Fuzzy clustering: A new approach for geostatistics analysis, *Int. J. Syst. Measure. Decisions* 2(2):13–23.

Bezdek, J. C., Ehrlich, R., and Full, W. E. (1984), FCM: The FUZZY C-MEANS clustering algorithm, *Comput. Geosci.* 10(2–3):191–203.

Chayes, F. (1970), On deciding whether trend surfaces of progressively higher order are meaningful, *Geol. Soc. Am. Bull.* 81:1273–1278.

Chorley, R. J., and Haggett, P. (1965), Trend surface mapping in geographical research, *Trans. Inst. Br. Geogr.* 37:47–67.

Davis, J. C. (1986), *Statistics and Data Analysis in Geology*, Wiley, New York, 646 pp.

Doveton, J. H., and Parsley, A. J. (1970), Experimental evaluation of trend surface distortions induced by inadequate data-point distributions, *Trans. Inst. Mining Metall.* 8: B197–B208.

Duda, R. O., and Hart, P. E. (1972), Use of the Hough transformation to detect lines and curves in pictures, *Commun.* ACM 15(1):11–15.

Fetterer, F. M., and Holyer, R. J. (1989), A Hough transform technique for extracting lead features from sea ice imagery, in *IGARSS '89, Proceedings of the 12th Canadian Symposium on Remote Sensing*, Vol. 2, pp. 1125–1128.

Fetterer, F. M., Pressman, A. E., and Crout, R. L. (1990), Sea ice lead statistics from satellite imagery on the Lincoln Sea during the ICESHELF acoustic exercise, Spring 1990, Naval Oceanographic and Atmospheric Research Laboratory, Stennis Space Center, MS, Technical Note 50, 8 pp.

Full, W. E., Ehrlich, R., and Bezdek, J. (1982), FUZZY QMODEL: A new approach for linear unmixing, J. *Math. Geol.* 14:1125–1128.

Harbaugh, J. W., and Merriam, D. F. (1968), *Computer Applications in Stratigraphic Analysis*, Wiley, New York, 282 pp.

King, L. J. (1969), *Statistical Analysis in Geography*, Prentice-Hall, Inc., Englewood Cliffs, NJ, 288 pp.

Koch, G. S., Jr., and Link, R. F. (1980), *Statistical Analysis of Geologic Data*, Dover, New York, 850 pp.

Kozo, T. L. (1983), Initial model results for arctic mixed layer cirulation under a refreezing lead, *J. Geophys. Res.* 88:2926–2934.

Martin, S., and Cavalieri, D. J. (1989), Contributions of the Siberian Shelf polynyas to the Arctic Ocean intermediate and deep water, *J. Geophys. Res.* 94:12725–12738.

Maykut, G. A. (1978), Energy exchange over young sea ice in the central arctic, *J. Geophys. Res.* 83(C7):3646–3658.

Maykut, G. A. (1982), Large-scale heat exchange and ice production in the central arctic, *J. Geophys. Res.* 87(C9): 7971–7984.

Poe, G. A., and Conway, R. W. (1990), A study of the geolocation errors of the Special Sensor Microwave / Imager (SSM / I), *IEEE Trans. Geosci. Remote Sens.* GE-28(5):791–799.

Shaus, R. H., and Galt, J. A. (1973), A thermodynamic model of an arctic lead, *Arctic* 26:208–221.

Smith, S. D., Muench, R. D., and Pease, C. H., (1990), Polynyas and leads: an overview of physical processes and environment, *J. Geophys. Res.* 95(C6):9461–9479.

Wang, J., and Howarth, P. J., (1989), Edge following as graph searching and Hough transform algorithms for lineament detection, in *IGARSS '89, Proceedings of the 12th Canadian Symposium on Remote Sensing*, Vol. 1, pp. 93–96.